

MODELS OF SKY BRIGHTNESS. S. I. Ipatov^{1,2,3}, K. Horne⁴, ¹Alsubai Est. for Scientific Studies, Doha, Qatar; ²Vernadsky Institute of Chemistry and Analytical Chemistry, Moscow, Russia; ³Space Research Institute, Moscow, Russia (siipatov@hotmail.com); ⁴Univ. of St. Andrews, St. Andrews, Scotland, United Kingdom.

Introduction: As one of steps of construction of the code for comparison of the exoplanet detection capability of microlensing observations for several telescopes [1], we analyzed models for sky brightness and seeing, calibrated by fitting to *I*-band data from the OGLE survey and RoboNet observations in 2011. This analysis can be interesting to different observers. In contrast to the previous papers (e.g., [2-6]) on sky brightness, we analyzed data from other telescopes and used χ^2 optimization for analysis of observations.

Observations analyzed: In our studies we analyzed observations made by the following telescopes:

1.3 m OGLE - The Optical Gravitational Lensing Experiment - Las Campanas, Chile.

2 m FTS - Faulkes Telescope South - Siding Springs, Australia.

2 m FTN - Faulkes Telescope North - Haleakela, Hawaii.

2 m LT - Liverpool Telescope - La Palma, Canary Islands.

For studies of sky brightness for FTS, FTN, and LT, we considered those microlensing events observed in 2011 for which the minimum number of light curve data points is greater than 15: FTS - 39 events; FTN - 19 events, LT - 20 events. For OGLE we considered 20 events (110251-110270).

Seeing: Our studies of seeing (FWHM in arcsec) are presented in Table 1 and Fig. 1. Table 1 contains the values of s_0 , s_1 , and σ obtained by χ^2 optimization of the straight line fit for seeing s vs airmass $a \approx \sec(z)$ (where z is the zenith distance): $s = s_0 + s_1(a-1)$ ($\chi^2 = \sum [(s_j - s_1(a_j-1) - s_0) / \sigma_s]^2$, where σ_s^2 is variance, the sum is for considered values of s_j at airmass a_j). Typical values of seeing for FTN were almost twice less than those for other three telescopes considered. For the three telescopes, typical values of seeing were about the same at airmass $a=1$, but at $a=2$ for OGLE they were smaller than those for FTS and LT.

Sky brightness vs. airmass: The used sky model was based mainly on [2]. For this model, the value of $I_{\text{sky}}(0)$ (I magnitude of sky brightness per square arcsec in zenith) was chosen in such a way that the sum of squares of differences between observational and model sky brightness magnitudes was minimum at this value of $I_{\text{sky}}(0)$ in the case when the Moon is below the horizon. The coefficients b_0 and b_{1o} presented in Table 2 were based on χ^2 optimization of the straight line fit ($b = b_{1o}(a-1) + b_0$, $\chi^2 = \sum [(b_j - b_{1o}(a_j-1) - b_0) / \sigma_b]^2$, σ_b^2 is variance, a is airmass, b_j is observational brightness at airmass a_j) for observations made at the Moon below

the horizon. The values $I_{\text{sky}}(0)$, b_0 and b_{1o} are presented for an extinction coefficient $e_{\text{xtmag}}=0.05$ (for e_{xtmag} equal to 0 and 0.1, values of $I_{\text{sky}}(0)$ differed by less than 0.3%). $I_{\text{sky}}(0)$ was 18.1 mag arcsec⁻² for OGLE, and it was greater for the other three telescopes considered.

Table 1. Seeing vs. airmass: $s = s_0 + s_1 \times (a-1)$

Telescope	FTS	FTN	LT	OGLE
s_0	1.33	0.68	1.35	1.33
s_1	0.52	0.21	0.42	0.29
σ	0.37	0.21	0.50	0.25

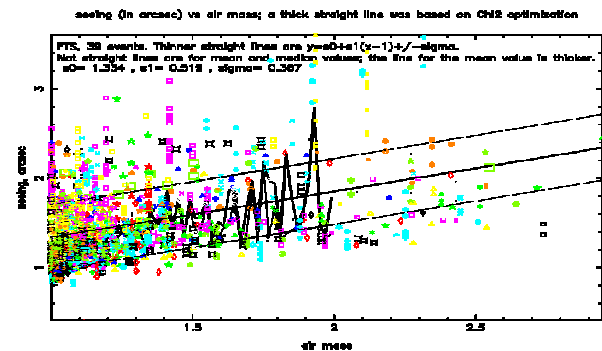


Fig. 1. Seeing (in arcsec) vs. airmass. FTS observations of 39 events. A thick straight line is based on χ^2 optimization ($y = s_0 + s_1(a-1)$, $s_0 = 1.334$, $s_1 = 0.519$). Thinner straight lines are $y = s_0 + s_1(a-1) \pm \sigma$ ($\sigma = 0.367$). Non-straight lines show mean and median values (the line for the mean value is thicker).

Using χ^2 optimization of the straight line fit $b = b_1(a-1) + b_{0i}$ and considering one value of b_1 for all events and different values of b_{0i} for different events, we calculated the length of the interval $\Delta b = \max\{b_{0i}\} - \min\{b_{0i}\}$ of values of b_{0i} . The values of b_{0i} characterize zenith sky brightness near different events. For observations made at the Moon below the horizon, $\Delta b \approx 1$ mag. An example of the plot of sky brightness vs. airmass, including lines $b = b_1(a-1) + b_{0i}$, can be found on http://presentations.copernicus.org/EPSC2013-331_presentation.pdf.

For different considered positions of the Moon and the Sun, the maximum values of b_{0i} (less bright sky) are almost the same as those for the Moon below the horizon. The difference in $\min\{b_{0i}\}$ (more bright sky) can be up to 1.5 mag for the different positions. The values of b_1 are presented in Table 2 for four restrictions on positions of the Moon and the Sun. Most of observations were made for airmass $a \leq 3$. The variation in sky brightness at $1 \leq a \leq 3$ does not exceed $|2b_1|$. For most

values of b_i presented in Table 2, $|2b_i| < 0.5$ mag. The values in Table 2 are presented for $t_{hruput} = 0.324$. The values of sky brightness obtained at two different values of t_{hruput} differed by $2.5 \log_{10}(t_{hruput2}/t_{hruput1})$, which is equal to 0.24 at $0.324/0.26 = 1.246$ (b_o is greater for a greater t_{hruput}).

Telescope	FTS	FTN	LT	OGLE
$I_{sky}(0)$ for Moon below horizon	19.0	18.7	19.6	18.1
b_o for Moon below horizon	18.8	18.3	19.0	18.0
b_{i_o} for Moon below horizon	-0.14	-0.13	-0.11	-0.22
b_i for Moon below horizon	-0.21	-0.18	-0.26	-0.24
b_i for all observations	-0.13	-0.26	-0.84	-0.24
b_i for solar elevation $\theta_{Sun} < -18^\circ$	-0.17	-0.18	-0.88	-0.24
b_i for Moon below & $\theta_{Sun} < -18^\circ$	-0.11	-0.22	-0.26	-0.23

The typical observational sky brightness near different events (regions of sky) at the same airmass usually varied (with events) by less than 1 mag if we analyze images with the Moon below the horizon and solar elevation $\theta_{Sun} < -18^\circ$. Analysis of observations shows that brightness of the sky can vary by up to 5-6 mag in the case of the bright Moon and the Sun close to the horizon. Such bright regions of the sky are not well simulated by the considered sky model, but often it is better not to observe such bright regions.

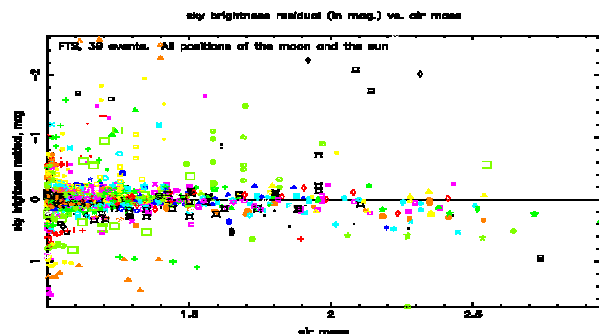


Fig. 3. Sky brightness residuals (mag) vs. airmass for the model with different b_{oi} for FTS observations of 39 events in the case of all positions of the Moon and the Sun.

Sky brightness residuals: Most of sky brightness residuals relative to the best fit model for each event (observations minus χ^2 optimization which is different for different events) are in a small range (-0.4 to 0.4 mag) even for all Moon and Sun positions; for the Moon below the horizon there are many values in the range [-0.2, 0.2]. Maximum values of sky brightness residuals for observations made at solar elevation $\theta_{Sun} < -18^\circ$ and for the Moon below the horizon usually are smaller by a factor of several than those for all observations (compare Figs. 3-4).

The influence of θ_{Sun} on sky brightness began to play a role at $\theta_{Sun} > -14^\circ$, and was considerable at $\theta_{Sun} > -7^\circ$. For example (see Fig. 5), if we consider only FTS observations with the Moon below the horizon, then sky brightness residual s_{br} can be up to -3 mag at $-8^\circ < \theta_{Sun} < -7^\circ$, $s_{br} > -1$ mag at $\theta_{Sun} < -8^\circ$, and $s_{br} > -0.4$ mag at $\theta_{Sun} < -14^\circ$.

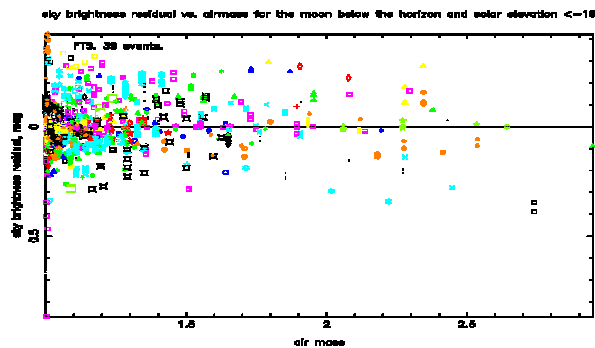


Fig. 4. Sky brightness residuals (mag) vs. airmass for the model with different b_{oi} for FTS observations of 39 events in the case when the Moon is below the horizon and solar elevation $\theta_{Sun} < -18^\circ$.

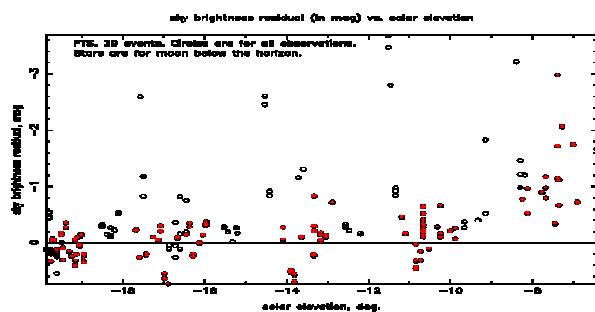


Fig. 5. Sky brightness residuals (in mag) vs. solar elevation for FTS observations of 39 events. Red signs are for the Moon below the horizon.

This publication was made possible by NPRP grant NPRP-09-476-1-78 from the Qatar National Research Fund (a member of Qatar Foundation). We are thankful to M. Hundertmark, M. Dominik, C. Snodgrass, R. Street, Y. Tsapras, D. Bramich, K. Alsbai, C. Liebig, for useful information.

References: [1] Ipatov S. I. et al. (2013) *Proc. IAU Symp. No. 293 "Formation, detection, and characterization of extrasolar habitable planets"*, ed. by N. Haghighipour, <http://arxiv.org/abs/1308.6159>, in press, [2] Krisciunas K. & Schaefer B. (1991) *PASP*, 103, 1033-1039. [3] Benn C. R. & Ellison S. L. (1998) *New Astronomy Reviews*, 42, 503-507. [4] Durisocoe D. M., Luginbuhl C. B., & Moore C. A. (2007) *PASP*, 119, 192-213. [5] Patat F. (2003) *A&A*, 400, 1183-1198. [6] Patat F. (2008) *A&A*, 481, 575-591.